Acta Geotechnica
https://doi.org/10.1007/s11440-024-02314-y

SHORT COMMUNICATION

Experimental investigations of water retention curves of fresh and decomposed municipal solid wastes under multiple drying and wetting cycles

Yuekai Xie[1] · Jianfeng Xue[1]

Received: 31 May 2023 / Accepted: 27 February 2024

Abstract
Municipal solid wastes (MSWs) disposed in landfills are generally exposed to drying and wetting cycles because of the variation in environmental conditions, decomposition of organics and leachate recirculation. This paper studies the water retention curves (WRCs) of fresh and degraded MSWs under various numbers of drying and wetting cycles with water and leachate exposure. The result indicates that the water retention capacities of MSWs decrease with drying and wetting cycles. The maximum hysteresis between the drying and wetting cycles is observed in the first cycles for all MSW samples. The WRCs of medium to highly decomposed MSWs under drying and wetting cycles are similar to those of soils. The WRCs of fresh MSWs can undergo substantial changes due to the discharge of intra-particle moisture caused by decomposition and compression. For both fresh and decomposed MSWs, the WRCs stabilize after 3 drying and wetting cycles. However, only the MSWs of one initial composition with similar void ratios were investigated. Further research should be conducted to investigate the water retention behavior of MSWs with diverse initial compositions (e.g., food contents) and void ratios.

Keywords Drying and wetting cycles · Leachate exposure · Municipal solid wastes · Water retention curves

1 Introduction

Municipal solid waste (MSW) disposed in landfills is generally exposed to drying and wetting loops due to the changes in the climate, leachate generation induced by decomposition, and leachate recirculation (bioreactor landfills). The content and distribution of moisture in MSWs can potentially affect the engineering properties of MSWs, such as the compression ratio and shear behavior, and thereby, the settlement and stability of landfills [38]. The high moisture contents due to inadequate management of leachate in landfills decrease the strength of MSWs and potentially cause slope failure [3]. The water retention curve (WRC) of MSWs is one of the most important factors affecting the design, operation, and management of landfills and gas and leachate collection systems [10, 26, 33].

The MSWs disposed in landfills are typically unsaturated. The unsaturated gas/liquid conductivity can be associated with the WRCs of MSWs [5]. In addition, the WRCs of MSWs vary with decomposition, which changes the pore size and distribution in the MSW matrix [26, 38]. To understand the efficiency of gas and leachate collection systems in unsaturated MSWs in landfills, a series of numerical simulations has been conducted [10, 29]. The results from the simulations are highly associated with the flow of gas and liquid in landfills. In landfills, MSWs can be desaturated due to gravity-induced drainage and saturated due to the recirculation and transportation of leachate [21]. However, in most of the current studies, only the drying phase of WRCs has been determined based on laboratory and field scale MSW samples [8, 19]. The results indicate that the WRCs of MSWs are significantly associated with the compression and degradation, which generally increase with the depth and age of MSWs [5]. The saturation (wetting) process of MSWs has not been

✉ Jianfeng Xue
jianfeng.xue@unsw.edu.au

[1] School of Engineering and Technology, the University of New South Wales, Canberra, ACT 2612, Australia

Published online: 15 April 2024

well studied. The knowledge of WRCs of MSWs under drying and wetting cycles needs to be extended.

One important behavior relevant to WRCs is hysteresis. Similar to soils exhibited in drying and wetting loops [2, 23], hysteretic behavior can also be observed in MSWs [26]. Under a given pressure head, MSWs can have two different moisture contents, i.e., one in the drying loops and the other one in the wetting loops. The hydraulic conductivity of MSWs increases with moisture contents and may also exhibit hysteretic behavior. The changes in the hydraulic conductivity influence the transportation of leachate and gas in landfills, and decomposition of MSWs [32]. The decomposition of MSWs is associated with the availability of moisture [31]. However, variations in the WRCs of MSWs during continuous drying and wetting loops have not been studied. Previous study carried by Kong et al. [16] suggests that the size and shape of the WRCs of soils after 2–3 cycles are almost identical because the major changes in the structure and volume of soils are likely to occur in first few drying and wetting cycles. In relatively fresh MSWs, the rapid release of intra-particle moisture after a slight degree of biodegradation (DOB) can affect the structures and moisture distribution in the MSWs [25] and thereby the WRCs. The variations in the WRCs of MSWs under drying and wetting cycles can therefore be different from that of the soils, especially after leachate exposure.

The objective of this study is to evaluate the effects of drying and wetting phases on fresh and degraded (up to 1080 days after decomposition) MSWs exposed to water and leachate. The degraded MSWs were prepared in bioreactors recirculated with leachate. The hysteresis of WRCs of MSWs with different DOBs during drying and wetting cycles was determined. The chemical properties of the outflow during the pressure plate tests were determined by inductively coupled plasma-optical emission spectrometry (ICP-OES).

2 Materials and methodology

2.1 Materials

The mature leachate was adopted in this study due to its relatively stable composition in comparison with the fresh leachate. The leachate was collected from a leachate pond located in the Mugga Lane Landfill, Canberra, Australia. The mature leachate retained in the pond was drained from landfill cells closed over 10 years [26]. The pH of the mature leachate (7.9) was similar to that of water. The chemical oxygen demand (COD) and ammonia concentration were measured by the potassium dichromate and salicylic acid methods [26, 31]. The mean values of COD and ammonia were 0.63 and 0.14 g/L, respectively.

The fresh MSWs were prepared from the MSWs in local bins in Canberra and soil samples from the landfill cover. The samples were characterized manually based on size (9.5 mm) and composition. The particles exceeding 9.5 mm were compressed or shredded, as suggested in previous studies [25, 26]. Fresh MSWs were generally compressed in landfills under the pressure of new lifts of MSWs or intermediate soil covers [27]. The relatively small size of 9.5 mm was selected because of the small diameter of the ring (50 mm) adopted for pressure plate experiments. For MSWs with larger particle sizes, modified apparatus was recommended, e.g., 150 mm diameter hanging column devices for maximum waste sizes of 25 mm [5]. The prepared MSWs were then remixed in accordance with the field composition investigated by Xie et al. [32], as presented in Table 1. The particle size distribution of prepared MSWs was similar to that of field MSWs after screening [32], as shown in Fig. 4d.

2.2 Sample preparation

The MSW samples with different decomposition durations were prepared in box shaped bioreactors with the size of 350 × 270 × 180 mm. The details of the bioreactor can be found in Xie and Xue [26]. To provide appropriate drainage, a gravel layer with a thickness of 20 mm was installed at the bottom of each bioreactor.

However, the dry unit weights or void ratios can significantly affect the WRCs of MSWs. For example, the increase in dry unit weights increased the air-entry pressures, residual moisture content of MSWs, and reduction in the slope of WRCs [5–8, 26]. Therefore, to minimize the effects of dry unit weights or void ratios and focus on the effects of biodegradation on the WRCs, the samples were prepared to different initial dry unit weights so that they

Table 1 Composition of fresh field and synthetic MSWs (wet basis)

Composition	Field (%)	Synthetic (%)
Soil	32.9	32
Paper and cardboard	19.3	19
Food and vegetation	17.6	17
Wood	8.1	9
Textiles	3.7	3
Glass	2.2	2
Plastics	11.0	11
Metal	0.4	1
Construction waste	4.7	6

could reach the same dry unit weight after different durations of biodegradation.

The prepared fresh MSWs were compacted with a standard proctor hammer until the final height of 120 mm and dry unit weights of 10.0 (MSW-F), 8.0 (MSW-M), and 6.0 kN/m^3 (MSW-H) were achieved. The abbreviations MSW-F, MSW-M, and MSW-H referred to the fresh, moderately degraded, and highly degraded MSWs, respectively. The dry unit weights of the MSWs were close to 10 kN/m^3 (9.61–10.35 kN/m^3) after 0 (MSW-F), 180 (MSW-M) and 1080 (MSW-H) days of decomposition, respectively. The specific gravity of samples ranged from 1.86 (MSW-F) to 1.93 (MSW-H). Therefore, after being decomposed for 0 (MSW-F), 180 (MSW-M) and 1080 (MSW-H) days, the void ratios of the MSWs prior to testing were similar. The influences of dry unit weight or initial void ratio on the WRCs of MSWs could be negligible, which were also out of the scope of this research. The dry unit weight and void ratio on the WRCs of MSWs after multiple drying and wetting should be further investigated.

Those compacted MSWs were then covered with 30 mm thick soils. In the first 10 weeks, 1.5 L leachate was recirculated into the bioreactor on a weekly basis. The frequency was reduced to half after 10 weeks (1.5 L/2 weeks). After 24 weeks, no leachate was recirculated. Before each recirculation, the leachate was collected from the drainage pipes. The temperature during the whole test period was maintained at 23 ± 2 °C. The corresponding DOBs of those samples were 0%, 26%, and 71% (Eq. (1)), respectively.

$$\mathrm{DOB} = \left(1 - \frac{X_{\mathrm{fi}}}{X_{\mathrm{fo}}}\right)\frac{1}{(1 - X_{\mathrm{fi}})} \tag{1}$$

where X_{fo} = the initial fraction of biodegradable components,

X_{fi} = the fraction of biodegradable components after partial decomposition.

2.3 Pressure plate tests

The decomposed samples were excavated from the bioreactors, followed by the saturation process in flexible-wall permeameters used by Xie et al. [28]. Fresh MSWs were permeated at the constant cell (15 kPa) and back pressure (10 kPa) for at least 72 h, with water or leachate. The degraded MSWs were saturated only with mature leachate under the same pressure sets. This was to minimize the impacts of pore liquids on the WRCs of MSWs.

The WRCs of MSWs were measured with pressure plate tests. The ring cutters in 50 mm diameter and 31.6 mm height were used to cut the saturated samples. The samples were then placed over high air-entry pressure (1500 kPa) ceramic disks. The samples were subjected to a vertical stress of 14 kPa. A digital displacement gauge was used to determine the displacement of MSWs during the drying and wetting loops, and the corresponding total volume of samples can be calculated. The suctions applied during the drying/wetting processes were 1, 2, 5, 10, 20, 50, 100, 200, and 500 kPa. When the change in each reading tube was within 1 mm (0.08 mL) in 12 h, the next step of matric suction was applied. A constant reading in 12 h under 500 kPa suggested the completion of one drying process, whereas that under 1 kPa indicated the completion of one wetting process. In one drying and wetting cycle, the applied suction increased from 1 to 500 kPa and reduced to 1 kPa.

Many models have been developed to describe the WRCs of soils [4, 22]. The Van Genuchten model (VGM) [22] has been widely used to describe the WRCs of MSWs [5, 20, 24, 26] and soils [16, 23]. Therefore, VGM was selected to compare the results with previous studies. The relationship between the volumetric moisture content and matric suction during both drying and wetting loops was fitted with VGM, as shown in Eq. (2).

$$\theta_{\mathrm{e}} = \frac{\theta - \theta_{\mathrm{r}}}{\theta_{\mathrm{s}} - \theta_{\mathrm{r}}} = \left[1 + \left(\frac{\psi}{\alpha}\right)^{n}\right]^{-m} \tag{2}$$

where θ_{e} = Effective saturation of MSWs at actual volumetric moisture content,

ψ = Matric suction of MSWs at actual volumetric moisture contents,

θ = Measured volumetric moisture contents of MSWs,

θ_{s} = Saturated volumetric moisture contents of MSWs,

θ_{r} = Residual volumetric moisture contents of MSWs,

m, n = Model parameters,

α = Air-entry pressures or wetting-saturation pressures of MSWs for drying and wetting loops, respectively.

2.4 ICP-OES

The microstructure of the MSW samples during drying and wetting cycles affected the hysteretic behavior [16]. The mercury intrusion porosimetry (MIP) tests were generally used to obtain the pore distribution. However, the high pressure applied during MIP tests can break soft MSW particles and open isolated pores, affecting the accuracy of pore distribution of MSWs [37]. Therefore, MIP may not be suitable for MSWs. To understand the biochemical behavior of MSWs during the drying and wetting process, the chemical properties of outflow from pressure plate tests after 6 cycles were determined with ICP-OES.

3 Results and discussion

3.1 WRCs of MSWs

The relationship between the volumetric moisture contents (VMC) of MSWs and matric suction during drying (D) and wetting (W) is presented in Fig. 1 (points). When fitting WRCs with VGM, the variation between the theoretical saturated volumetric moisture content and the determined volumetric moisture content is neglected. Although gravity-induced drainage occurs during sample preparation [4, 20], most of the air voids could be excluded during the application of the vertical loading [26]. The determined saturated moisture contents are close to the theoretical saturated moisture contents calculated based on phase relationship (within 2% of difference). This suggests that the samples can be saturated using the saturation method. Therefore, the saturated moisture contents determined during the tests are used, as recommended in a previous study [26].

3.2 Effects of drying and wetting cycles

The fitting parameters and fitted curves are shown in Table 2 and Fig. 1 (the solid lines), respectively. Figure 2 shows the correlation between the effective saturation and matric suction, together with the fitted curves using the parameters in Table 2. The trend of effective saturation and volumetric moisture content with matric suction is similar. The difference between the curves in Figs. 1 and 2 mainly results from the reduction in the saturated moisture contents due to the decrease in void ratios with drying and wetting cycles. Figure 3 presents the changes in those parameters with the number of drying and wetting cycles adopted. The figure also compares the parameters of a granite residual soil (GRS) [16], and an artificially mixed soil from a silicon micro-powder (SMP) [23]. The results shown in Fig. 3 indicate that saturated and residual moisture contents or moisture retention capacities of MSWs decrease as the number of drying and wetting cycles increases. Such reduction is similar to that of soils under

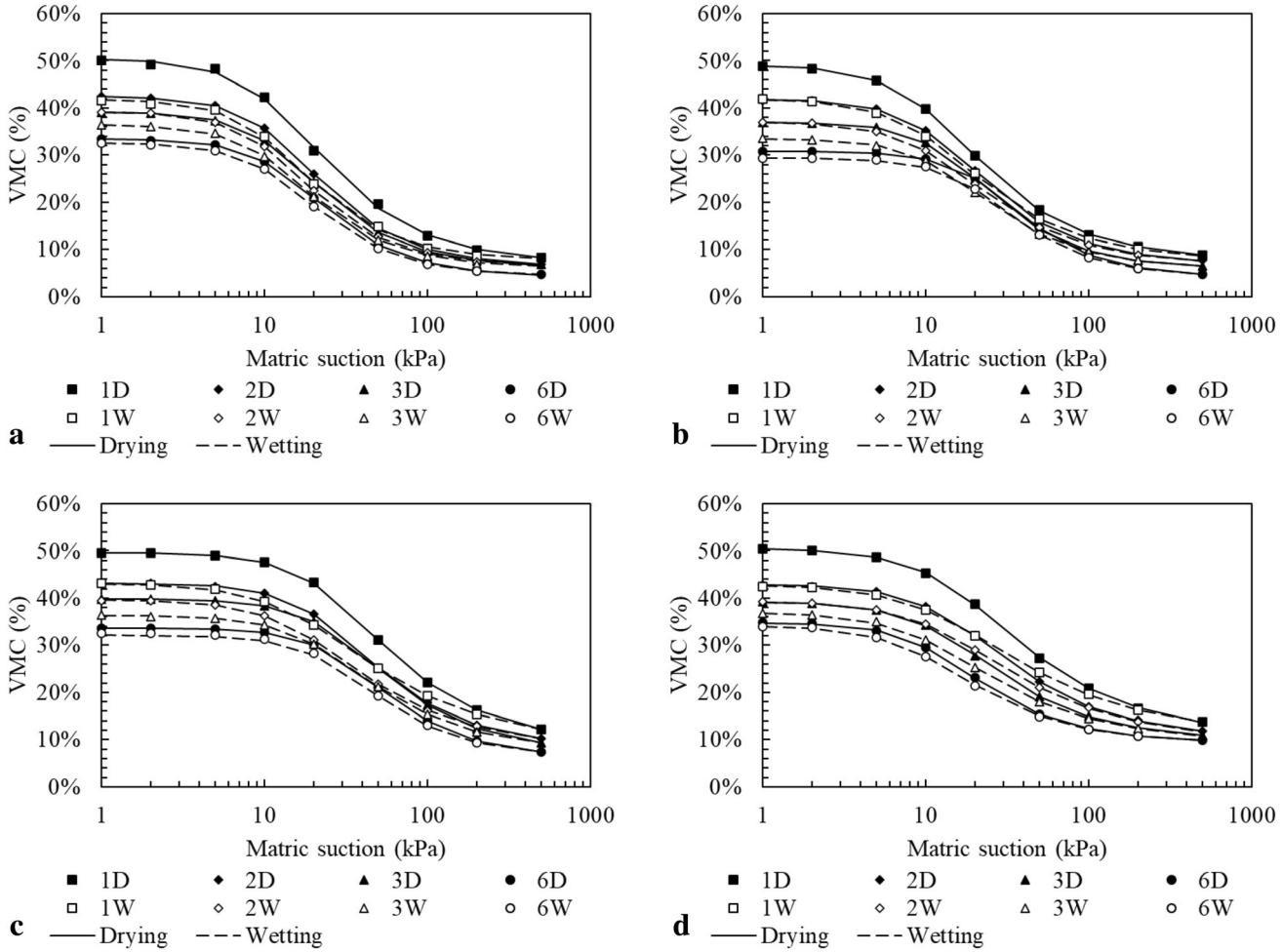

Fig. 1 WRCs of the MSWs after different cycles of drying and wetting with water or leachate (*VMC*: Volumetric moisture content): (**a**) MSW-F, water exposure, (**b**) MSWF, leachate exposure, (**c**) MSW-M, leachate exposure, (**d**) MSW-H, leachate exposure

Table 2 VGM parameters of MSWs after different cycles of drying and wetting by water or leachate

Test group	Cycles	Drying				Wetting			
		α (kPa)	θ_s (%)	θ_r (%)	n	α (kPa)	θ_s (%)	θ_r (%)	*n*
MSW-F (W)	1	13.7	50.3%	7.0%	1.97	12.3	41.8%	7.6%	2.16
	2	14.2	42.5%	6.4%	2.15	12.6	39.2%	6.3%	2.18
	3	14.3	39.1%	6.2%	2.17	12.9	36.4%	6.2%	2.20
	6	15.4	33.4%	4.3%	2.22	13.8	32.5%	4.3%	2.20
MSW-F (L)	1	12.2	49.0%	7.5%	1.93	12.0	41.9%	7.5%	1.92
	2	14.0	41.8%	6.7%	2.03	13.2	37.1%	6.7%	1.97
	3	16.7	37.0%	6.0%	2.17	14.9	33.5%	5.9%	2.06
	6	26.5	30.7%	4.1%	2.29	23.1	29.3%	4.3%	2.24
MSW-M (L)	1	31.1	49.6%	9.3%	1.94	19.2	43.2%	8.6%	1.70
	2	27.8	43.2%	8.2%	1.99	19.9	39.7%	8.0%	1.83
	3	32.9	39.8%	7.2%	2.01	25.1	36.4%	7.5%	1.92
	6	35.4	33.7%	6.0%	2.15	31.3	32.1%	6.1%	2.11
MSW-H (L)	1	17.7	50.5%	10.7%	1.78	14.0	42.8%	10.4%	1.64
	2	16.7	42.8%	10.0%	1.85	14.7	39.3%	9.5%	1.73
	3	14.6	39.3%	9.6%	1.89	12.3	36.9%	9.3%	1.79
	6	13.1	34.9%	9.2%	2.04	10.7	34.1%	9.2%	1.94

continuous drying and wetting cycles, as shown in Fig. 3a, b. This could be attributed to the breakdown of bonding structures, decrease in the pore volume, and formation of cracks during the drying and wetting cycles [18], as well as the ink-bottle effect, contact angle effect, entrapped air, and swelling [15]. The bonding effect would be weakened due to the loss of cementitious components due to continuous leachate exposure [17]. The cementation is destroyed due to stress concentration induced by the absorption and desorption [34]. Xu et al. [34] also indicate that the structure of soil particles in MSWs can be converted from shelf structures to polymer structures under drying-wetting cycles. Additionally, cracks can occur during the drying processes. Continuous drying-wetting cycles can extend the dimensions of those cracks and generate new cracks [16]. Those effects mentioned above decrease the water retention capacity of MSWs.

It is noticeable that the decrease in the saturated and residual moisture content of MSWs is higher than those of soils. This can be mainly attributed to the entrapped air. The macro-pores can retain water when surrounded by micro-pores but cannot retain water once been dried prior to wetting. The air is likely to occupy the volume of the moisture in the macro-pores with the outflow water and potentially block the micro-pores due to air bubbles, forming more macro-pores. The generation of landfill gas due to the decomposition of MSWs during drying and wetting can enhance the entrapped air effect.

The WRCs of the MSWs reach a nearly stable condition after 3 drying and wetting cycles. This means the structure of the MSWs could have been stabilized after 3 cycles. The effects of leachate recirculation on particle rearrangement within the MSW matrix could be more significant in the first few times of recirculation, and further recirculation may only provide a suitable environment for mechanical compression and biodegradation. Xie et al. [31] investigated the long-term settlement of MSWs with similar composition over 2 years. The experiments were performed in laboratory-scale bioreactors with recirculation of mature leachate. The results suggest that the majority of settlement and reduction in void ratios occurs during the first 3 cycles of leachate recirculation and collection (wetting and drying) due to particle rearrangement and release of intra-particle water. Further recirculation of mature leachate enhances the decomposition of MSWs and increases the compression index due to the increase in pH [30].

3.3 Effects of pore liquids

The comparison between the WRCs of MSWs exposed to water and leachate (Fig. 1a, b) indicates that the leachate exposure does not have substantial influences on the initial WRCs of fresh MSWs. The smaller *n* value during the wetting process of MSWs indicates that the distribution of the pore size in the samples exposed to leachate is less uniform compared to those exposed to water. The ions contained in the leachate can result from the construction wastes, metals, sludges, and solidified/stabilized soils [11, 12]. Those ions, such as Cl^-, SO_4^{2-}, and CO_3^{2-} could

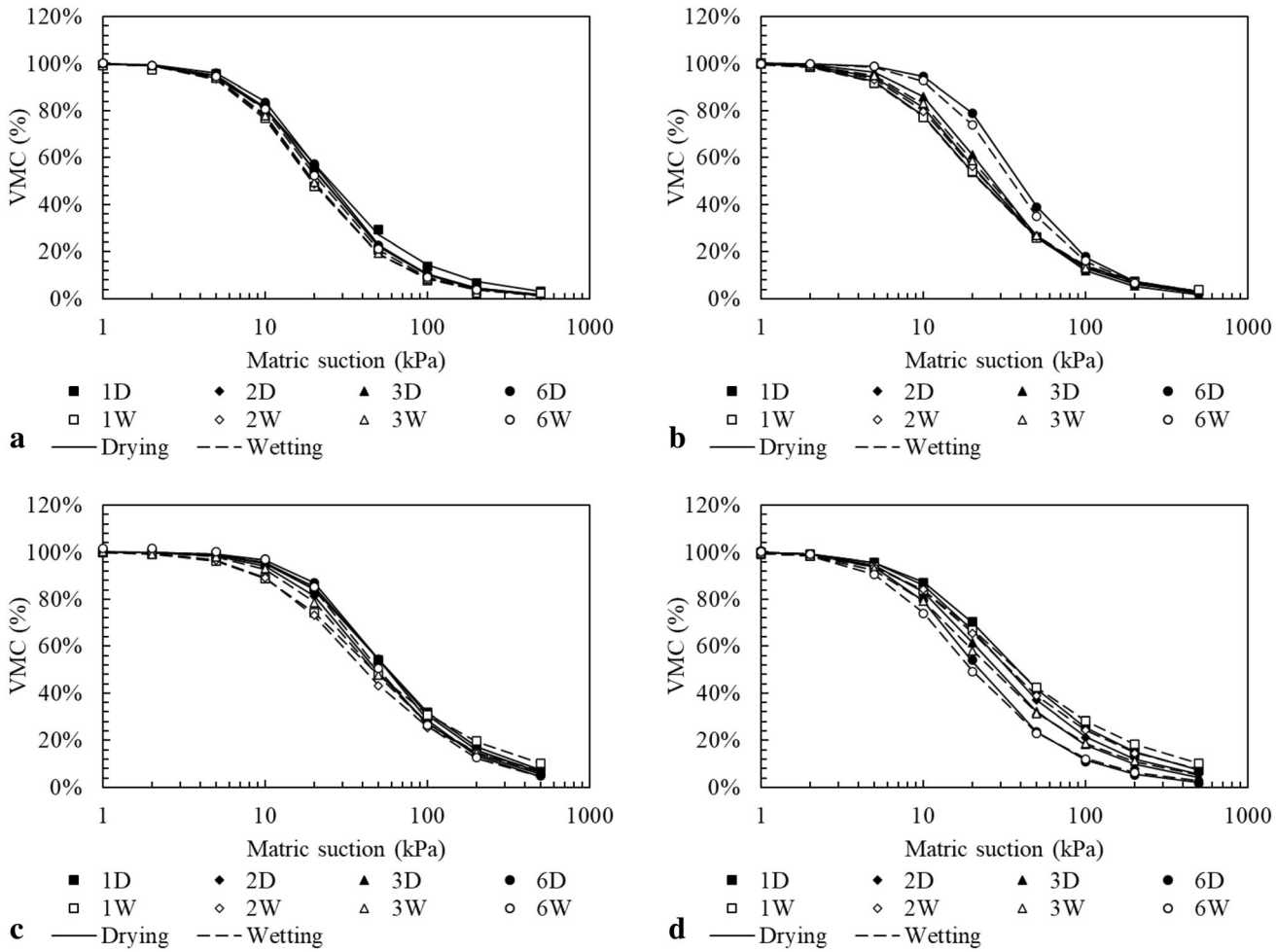

Fig. 2 WRCs of the MSWs after different cycles of drying and wetting with water or leachate (Effective saturation): (**a**) MSW-F, water exposure, (**b**) MSW-F, leachate exposure, (**c**) MSW-M, leachate exposure, (**d**) MSW-H, leachate exposure

react quickly with the cementitious components within the MSWs [17]. This could result in looser structures in the MSWs induced by the separation and dispersion of MSW solids, i.e., the less uniform pore size distribution with higher pore sizes. This is consistent with the ICP results shown in Table 3. The existence of Ca in the matrix contributes to the formation of a strong bond between fine MSW particles [9]. The reduction in Ca in the matrix causes a loose and dispersed structure.

In addition, the leachate exposure only has a minimal effect on the WRC parameters of MSWs under drying and wetting cycles, except for air-entry pressures. As the number of drying and wetting cycles increases, the air-entry pressures of the samples exposed to leachate exhibit a more significant rise in contrast to those exposed to water. This can be attributed to the formation of biofilm within the MSW matrix. The biofilm is associated with soils' biochemical processes and can be enhanced by leachate exposure [1]. The biofilm can grow on the surface of both macro and micro-pores, clogging the voids in the MSWs matrix. The clogging induced by biofilm formation effectively reduces the maximum sizes of macro-pores and potentially decreases the mean dimensions of pores in the MSW matrix [28]. The reduction in pore sizes increases the air-entry pressures of MSWs. The air-entry pressures of fresh MSWs increase with the number of drying and wetting cycles, especially under leachate exposure. This is opposite to the natural or artificially mixed soils reported in the literature [14, 23].

Unlike soil materials, changes in the WRCs of MSWs also result from the differences in the nature of the waste constitutions. The decrease in saturated moisture contents after 6 cycles is slightly higher in the fresh MSWs. This is attributed to the discharge of intra-particle moisture. The intra-particle moisture held within the waste constitutions, such as food, is initially not able to transport freely in the MSW matrix. However, this intra-particle moisture can be easily squeezed out when subjected to stress or

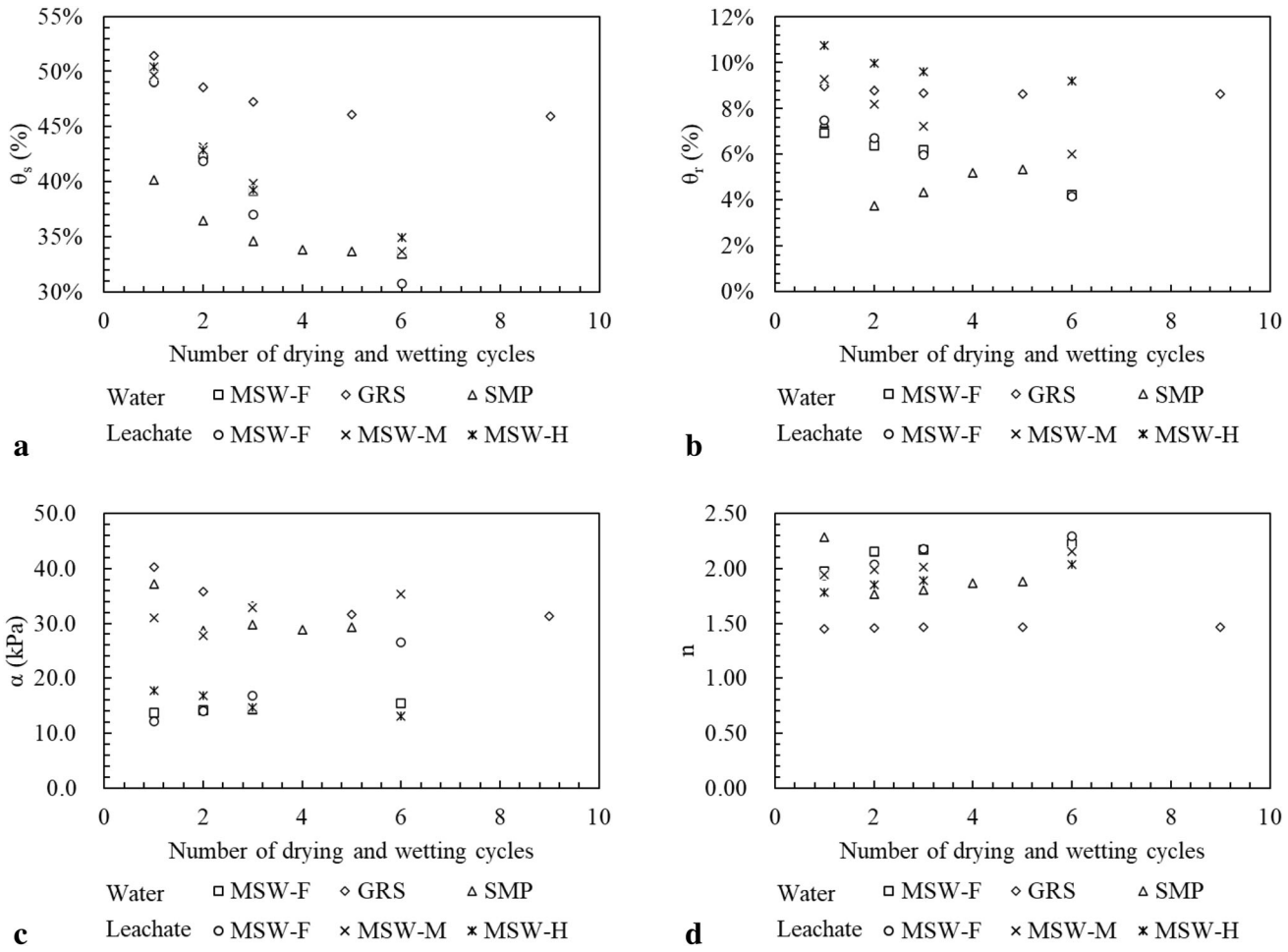

Fig. 3 Variation in the WRC parameters (drying phase) of MSWs with drying and wetting cycles: (**a**) Saturated moisture content θ_s, (**b**) Residual moisture content θ_r, (**c**) Air-entry pressure α, (**d**) Model parameter n

Table 3 Elemental composition of outflow from the pressure plate tests

Analyte	W			L		
	Raw	MSW-F	MSW-H	Raw	MSW-F	MSW-H
Na	10.5	16.2	22.5	323.5	369.8	380.4
Mg	3.6	9.3	11.0	77.3	97.3	97.8
K	1.8	5.1	6.1	52.3	68.0	74.9
Ca	3.3	42.9	51.0	33.4	189.2	246.7

decomposition [31], but cannot be adsorbed back once being removed. As MSWs continue to decompose, the intra-particle water retained in MSWs decreases. The WRCs of decomposed MSWs subjected to drying and wetting cycles become closer to those of the soil. The reduction of saturated and residual moisture contents of decomposed MSWs is lower compared to those of fresh MSWs. The air-entry pressures decrease with the number of drying and wetting cycles, as can be seen in Fig. 3a–d and Table 2.

3.4 Effects of decomposition

The WRCs of MSWs are influenced by the degrees of biodegradation (DOB), as shown in Fig. 4. The residual volumetric moisture contents, air-entry pressures, and model parameter *n* of MSWs vary with the DOBs. The residual moisture content of MSWs is a function of the balance between organic contents (e.g., paper) and highly degraded organic fractions [24]. The reductions in organic fractions of MSWs such as paper reduce the moisture retention capacity of MSWs while increased percentages of decomposed fine particles enhance the moisture retention capacity. As MSWs decompose, the sizes of degradable particles reduce, and the maximum pore size within the MSWs could potentially increase or decrease, depending on DOBs. The reduction in the overall pore dimensions contributes to higher air-entry pressure and residual moisture content. This can be partially reflected by the reduction in the particle size shown in Fig. 4d. The percentage of fine

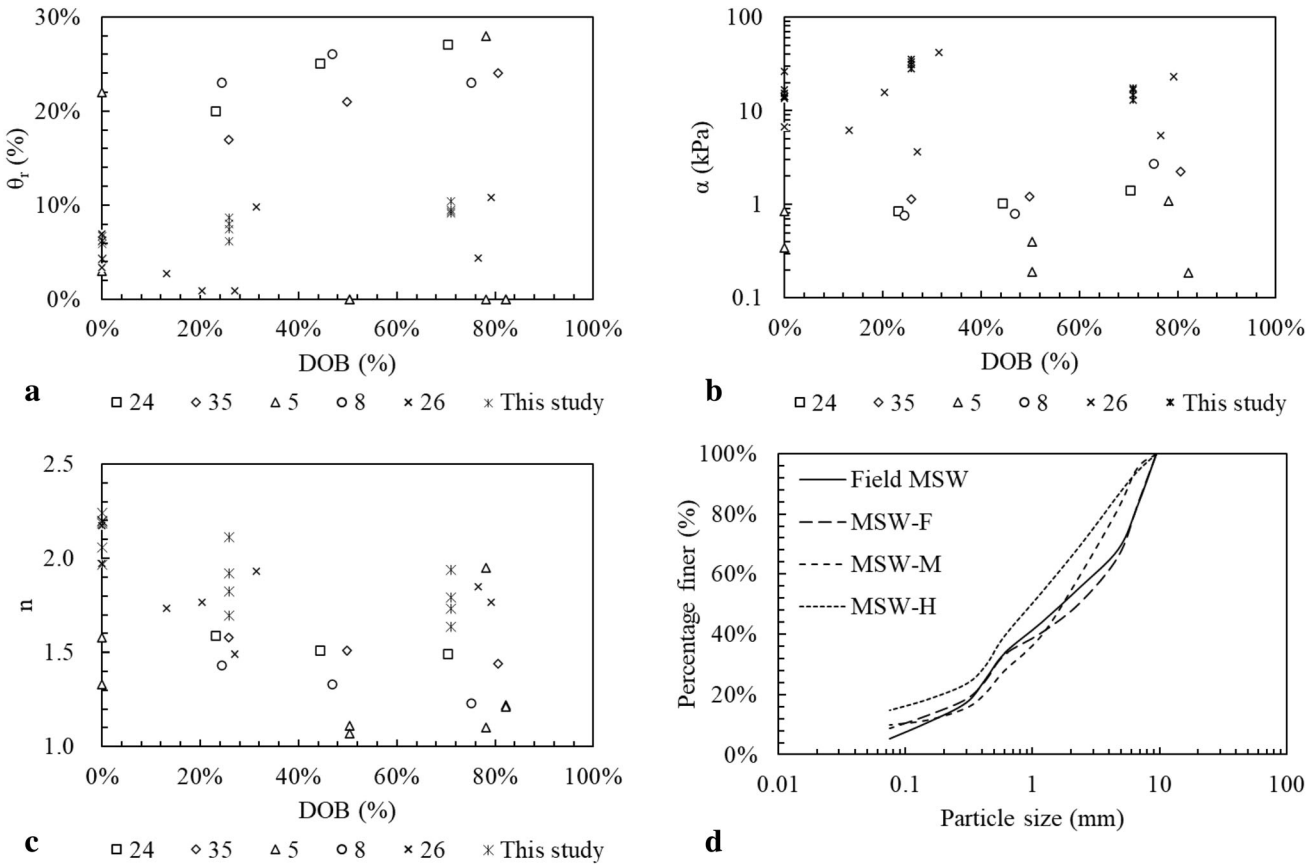

Fig. 4 Variation in the WRC parameters (drying phase) and particle size of MSWs with decomposition: (**a**) Residual moisture content θ_r, (**b**) Air-entry pressure α, (**c**) Model parameter n, (**d**) Particle size distribution

contents increases with DOB as the particle size distribution curve moves to the left.

Although there is no clear relationship between overall residual moisture content/air-entry pressure and DOB, for each individual study, the residual moisture content and air-entry pressure increase with DOB. Those changes are associated with the reduction in particle sizes due to decomposition. The increase in the fine content potentially decreases the pore dimensions [5], increases the number of micro-pores, and creates a more uniform pore size distribution [26]. Zhang et al. [37] also evaluated the pore size distribution of MSWs with different DOBs. The MSWs with higher DOBs exhibit lower volumes of macro-pores (> 5 μm) compared to those with lower DOBs. This is consistent with the increase and then decrease in air-entry pressures and model parameter *n* as the MSWs decompose from fresh to moderately (180 days) and then to highly (1080 days) decomposed as shown in Fig. 3c, d.

3.5 Effects of compression

Another important factor affecting the WRCs of the MSWs during the drying and wetting cycles is compression, which increases the dry unit weight of MSWs. The dry unit weight of MSWs increases during drying and wetting loops. The influences of dry unit weight on the WRCs of MSWs have been extensively studied in previous studies [5, 26, 35]. Figure 5 compares the WRC parameters under different dry unit weights. The air-entry pressures and residual moisture contents increase with the dry unit weight of MSWs (Fig. 5a, b). The model parameter *n* decreases with the dry unit weight of MSWs (Fig. 5c). This is attributed to the decrease in pore sizes and uniform pore size distribution due to increased dry unit weight [5].

Although the air-entry pressure of fresh and moderately decomposed MSWs increases with the dry unit weight induced by compression during dry and wetting, the increase is much more significant compared to MSWs compacted to different initial dry unit weights. Additionally, different trends in residual moisture contents and model parameter *n* can be observed from MSWs with different dry unit weights induced by drying-wetting cycles. This suggests that the increase in dry unit weight due to compression may not be the main cause of changes in the WRC parameters with drying and wetting loops.

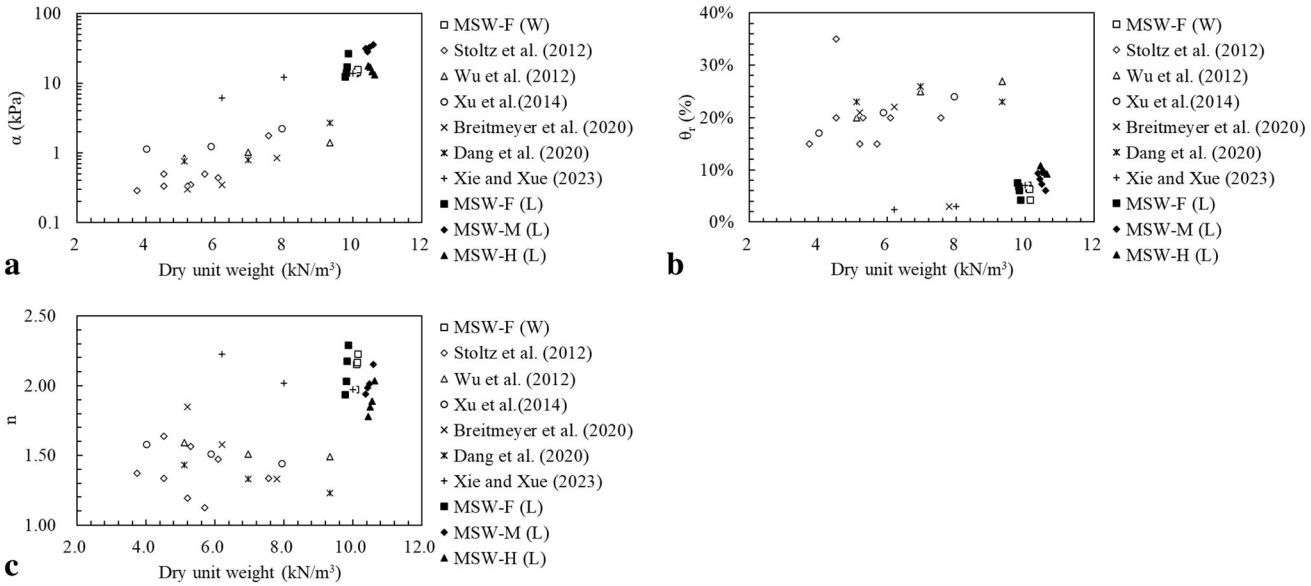

Fig. 5 Effects of dry unit weight on WRC of MSWs: (**a**) Air-entry pressure α, (**b**) Residual moisture content θ_r, (**c**) Model parameter n

3.6 Hysteresis of MSWs

Similar hysteresis loop of MSWs and soils can be observed [16]. This can be attributed to ink-bottle effects, contact angle effects and entrapped air effects [14]. The hysteresis of MSWs between drying and wetting loops of MSWs is quantified using Eq. (3) [15].

$$\text{Hysteresis} = \int_{0.1}^{500} \theta_{\text{drying}} \mathrm{d}\psi - \int_{0.1}^{500} \theta_{\text{wetting}} \mathrm{d}\psi \tag{3}$$

The hysteresis of the MSW samples during the drying and wetting phases is presented in Fig. 6. For both fresh and decomposed MSWs, the maximum hysteresis is measured in the first loop of drying and wetting due to the relatively large pores in the MSW matrix. Due to the high suction applied during drying cycles, significant volume change could occur during the first drying cycle, which results in smaller voids in the MSWs. A relatively smaller hysteresis can therefore be observed after the first drying and wetting cycle. As the number of drying and wetting cycles increases, MSWs gradually perform like a passive system, where no further adsorption and desorption of moisture can be observed, as also shown in existing study on soils [16]. However, this method only quantifies the hysteresis behavior of MSWs. The effects such as contact angles between solids and liquids and ink-bottle have not been investigated. Although the contact angle is generally assumed to be constant during the drying and wetting processes, it can be larger during the wetting process and may change with the particle roughness and temperature due to the decomposition of MSWs [13]. The ink-bottle

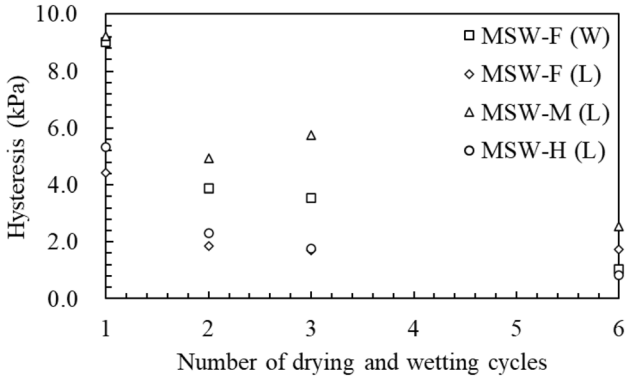

Fig. 6 Hysteresis of MSWs subjected to different numbers of drying and wetting cycles

effect results from the non-homogeneous shapes and sizes of interconnected pores [39] and can be quantified by the pore size distribution function and arrangement of dry and wet pores [36]. The desaturation of pores occurs under the high snap-off suction value and is dependent on the smaller section at the bottle neck [2]. By contrast, the pores are saturated under the low snap-off suction, and this process is dominant by the large section in the bottle body. The micro-pores can remain dry with the reduction in suction during the wetting process due to the block of water flow by the macro-pores [36]. The shapes and dimension of pores of MSWs vary with the compression and decomposition [26], affecting the ink-bottle effect and contact angle of MSWs. Further studies can be conducted to investigate the applicability of unsaturated soil models for MSWs [39, 40].

4 Conclusion

This study investigated the effects of drying and wetting cycles on the water retention curves (WRCs) of municipal solid wastes (MSWs). The MSW samples with various degrees of degradation were prepared in the laboratory. Up to 6 drying and wetting cycles were adopted with the maximum matric suction of 500 kPa. The liquids used for the tests were water (fresh MSWs) and leachate (fresh and degraded MSWs). The results indicate that the water retention capacity of MSWs decreases as the number of drying and wetting increases. The maximum hysteresis is obtained in the first drying and wetting cycle. The WRCs of the MSWs tend to stabilize after 3 drying and wetting cycles. As the number of drying and wetting loops increases, water retention behavior of the decomposed MSWs is close to those of soils. The air-entry pressures decrease, but the model parameter n increases with the number of drying and wetting cycles. The water retention behavior of MSWs can be affected by the degree of biodegradation and mechanical compression, which results in the discharge of intra-particle moisture from the MSWs. The leachate exposure does not greatly affect the WRC parameters of the MSWs under drying and wetting loops, except for air-entry pressures. The air-entry pressure of the fresh MSWs increases with the number of drying and wetting cycles, especially under leachate exposure.

Acknowledgements This project was financially supported by ACT NOWaste. The support from School of Engineering and Technology, University of New South Wales was acknowledged.

Funding Open Access funding enabled and organized by CAUL and its Member Institutions.

References

1. Aldaeef A, Rayhani MT (2014) Hydraulic performance of Compacted Clay Liners (CCLs) under combined temperature and leachate exposures. Waste Manage 34:2548–2560
2. Bate B, Nie S, Chen Z, Zhang F, Chen Y (2021) Construction of soil–water characteristic curve of granular materials with toroidal model and artificially generated packings. Acta Geotech 16:1949–1960
3. Blight G (2008) Slope failures in municipal solid waste dumps and landfills: a review. Waste Manage Res 26:448–463
4. Breitmeyer RJ, Benson CH (2014) Evaluation of parameterization techniques for unsaturated hydraulic conductivity functions for municipal solid waste. Geotech Test J 37:1–16
5. Breitmeyer RJ, Benson CH, Edil TB (2020) Effect of changing unit weight and decomposition on unsaturated hydraulics of municipal solid waste in bioreactor landfills. J Geotechn Geoenviron Eng 146:04020021
6. Cai G, Zhou A, Liu Y, Xu R, Zhao C (2020) Soil water retention behavior and microstructure evolution of lateritic soil in the suction range of 0–286.7 MPa. Acta Geotech 15:3327–3341
7. Cai G, Liu Y, Zhou A, Li J, Yang R, Zhao C (2022) Temperature-dependent water retention curve model for both adsorption and capillarity. Acta Geotech 17:5157–5186
8. Dang M, Chai J, Xu Z, Qin Y, Cao J, Liu F (2020) Soil water characteristic curve test and saturated-unsaturated seepage analysis in Jiangcungou municipal solid waste landfill. China Eng Geol 264:105374
9. Demdoum A, Gueddouda MK, Goual I, Souli H, Ghembaza MS (2020) Effect of landfill leachate on the hydromechanical behavior of bentonite-geomaterials mixture. Constr Build Mater 234:117356
10. Feng S, Fu W, Zhou A, Lyu F (2019) A coupled hydro-mechanical-biodegradation model for municipal solid waste in leachate recirculation. Waste Manage 98:81–91
11. Feng Y-S, Du Y-J, Zhou A, Zhang M, Li J-S, Zhou S-J, Xia W-Y (2021) Geoenvironmental properties of industrially contaminated site soil solidified/stabilized with a sustainable by-product-based binder. Sci Total Environ 765:142778
12. Feng Y-S, Zhou S-J, Zhou A, Xia W-Y, Li J-S, Wang S, Du Y-J (2022) Reuse of a contaminated soil stabilized by a low-carbon binder as roadway subgrade material and mechanical performance evaluation. Eng Geol 303:106656
13. Fu Y, Liao H, Chai X, Li Y, Lv L (2021) A hysteretic model considering contact angle hysteresis for fitting soil-water characteristic curves. Water Res Res. https://doi.org/10.1029/2019WR026889
14. Gallage C, Kodikara J, Uchimura T (2013) Laboratory measurement of hydraulic conductivity functions of two unsaturated sandy soils during drying and wetting processes. Soils Found 53:417–430
15. Gallage CPK, Uchimura T (2010) Effects of dry density and grain size distribution on soil-water characteristic curves of sandy soils. Soils Found 50:161–172
16. Kong L, Sayem HM, Tian H (2018) Influence of drying–wetting cycles on soil-water characteristic curve of undisturbed granite residual soils and microstructure mechanism by nuclear magnetic resonance (NMR) spin-spin relaxation time (T 2) relaxometry. Can Geotech J 55:208–216
17. Li J, Xue Q, Wang P, Liu L (2013) Influence of leachate pollution on mechanical properties of compacted clay: a case study on behaviors and mechanisms. Eng Geol 167:128–133
18. Sayem HM, Kong LW (2016) Effects of drying-wetting cycles on soil-water characteristic curve. In: Proceedings of the International Conference on Power Engineering & Energy, Environment, Shanghai, China, pp 21–23
19. Shi J, Wu X, Ai Y, Zhang Z (2018) Laboratory test investigations on soil water characteristic curve and air permeability of municipal solid waste. Waste Manage Res 36:463–470
20. Stoltz G, Tinet A-J, Staub MJ, Oxarango L, Gourc J-P (2012) Moisture retention properties of municipal solid waste in relation to compression. J Geotechn Geoenviron Eng 138:535–543

21. Tinet A, Oxarango L, Bayard R, Benbelkacem H, Stoltz G, Staub M, Gourc J-P (2011) Experimental and theoretical assessment of the multi-domain flow behaviour in a waste body during leachate infiltration. Waste Manage 31:1797–1806
22. Van Genuchten MT (1980) A closed-form equation for predicting the hydraulic conductivity of unsaturated soils. Soil Sci Soc Am J 44:892–898
23. Wen T, Shao L, Guo X, Zhao Y (2020) Experimental investigations of the soil water retention curve under multiple drying–wetting cycles. Acta Geotech 15:3321–3326
24. Wu H, Wang H, Zhao Y, Chen T, Lu W (2012) Evolution of unsaturated hydraulic properties of municipal solid waste with landfill depth and age. Waste Manage 32:463–470
25. Xie Y (2022) Experimental and Numerical Assessment of Geotechnical and Settlement Behaviours of Municipal Solid Wastes with a Special Reference to Mugga Lane Landfill. In: PhD Thesis, University of New South Wales
26. Xie Y, Xue J (2023) Experimental investigation of water retention curves of municipal solid wastes with different paper contents, dry unit weights and degrees of biodegradation. Waste Manage 163:73–84
27. Xie Y, Xue J, Gnanendran CT (2018) Model Uncertainties in Long-Term Settlement Prediction of Landfill Waste. In: Proceedings of the 8th International Congress on Environmental Geotechnics, pp 127–134
28. Xie Y, Xue J, Gnanendran CT (2022) Effect of landfill leachate on hydraulic properties of an organic soil. In: 7th International Young Geotechnical Engineers Conference, Sydney, Australia, pp 277-284
29. Xie Y, Xue J, Deane A (2023) Numerical modelling of settlement of municipal solid waste in landfills coupled with effects of biodegradation. Waste Manage 163:108–121
30. Xie Y, Xue J, Gnanendran CT, Xie K (2022) Geotechnical properties of fresh municipal solid wastes with different compositions under leachate exposure. Waste Manage 149:207–217
31. Xie Y, Xue J, Gnanendran CT, Xie K (2023) Physical, geotechnical and biochemical behaviours of municipal solid waste in field and laboratory bioreactors. Waste Manage 159:39–51
32. Xie Y, Wang H, Guo Y, Wang C, Cui H, Xue J (2023) Effects of biochar-amended soils as intermediate covers on the physical, mechanical and biochemical behaviour of municipal solid wastes. Waste Manage 171:512–521
33. Xie Y, Wang H, Chen Y, Guo Y, Wang C, Cui H, Xue J (2023) Water retention and hydraulic properties of a natural soil subjected to microplastic contaminations and leachate exposures. Sci Total Environ. https://doi.org/10.1016/j.scitotenv.2023.166502
34. Xu X-t, Shao L-j, Huang J-b, Xu X, Liu D-q, Xian Z-x, Jian W-b (2021) Effect of wet-dry cycles on shear strength of residual soil. Soils Found 61:782–797
35. Xu XB, Zhan LT, Chen YM, Beaven RP (2014) Intrinsic and relative permeabilities of shredded municipal solid wastes from the Qizishan landfill, China. Can Geotech J 51:1243–1252
36. Zhai Q, Rahardjo H, Satyanaga A, Dai G, Du Y (2020) Estimation of the wetting scanning curves for sandy soils. Eng Geol 272:105635
37. Zhang W, Lin M (2019) Evaluating the dual porosity of landfilled municipal solid waste. Environ Sci Pollut Res 26:12080–12088
38. Zhao R, Zhou A, Yao Y-P (2022) Interpretation of mechanical and biodegradation behaviour of municipal solid waste. Comput Geotech 150:104927
39. Zhou A-N (2013) A contact angle-dependent hysteresis model for soil–water retention behaviour. Comput Geotech 49:36–42
40. Zhou A-N, Sheng D, Sloan SW, Gens A (2012) Interpretation of unsaturated soil behaviour in the stress–saturation space, I: volume change and water retention behaviour. Comput Geotech 43:178–187